Low-dimensional dynamics and bifurcations in oscillator networks via bi-orthogonal spectral decomposition

2000 J. Phys. A: Math. Gen. 33 3555

(http://iopscience.iop.org/0305-4470/33/18/303)

J. Phys. A: Math. Gen. **33** (2000) 3555–3566. Printed in the UK PII: S0305-4470(00)09233-7

Low-dimensional dynamics and bifurcations in oscillator networks via bi-orthogonal spectral decomposition

J Schwarz†‡, K Bräuer†, G Dangelmayr§ and A Stevens‡

† Institut für Theoretische Physik, Universität Tübingen, Auf der Morgenstelle 14, D-72076 Tübingen, Germany

‡ Universitätsklinik für Psychiatrie und Psychotherapie, Osianderstrasse 24, D-72076 Tübingen, Germany

§ Department of Mathematics, Colorado State University, 121 Engineering Building, Ft Collins, CO 80523, USA

Received 2 November 1999, in final form 7 March 2000

Abstract. Many natural neural systems are functionally or hierarchically organized into interacting ensembles of neural populations. To investigate the dynamics in a hierarchical system of coupled bistable van der Pol oscillators we apply the bi-orthogonal decomposition into empirical orthogonal spatial and temporal modes. Within this method the dynamics and synchronized patterns are characterized by global, temporal and spatial entropy and energy. Different states of the network activity are identified as synchronous or asynchronous dynamics induced by external periodic input. Of particular interest is the ability of the bi-orthogonal decomposition to detect bifurcations following variations of the system parameter. Bifurcations correspond to crossings of the eigenvalues where an exchange of dominant modes takes place. In our simulations we observe a bifurcation induced by variations of input frequency and strength, identified as a saddle-node bifurcation of the unstable/stable pair of limit cycles.

1. Introduction

In systems of identical or nearly identical interacting subsystems cooperative and competitive phenomena are observed that are emergent properties of the system. Of particularly interest are systems based on analogies with neural networks. Their neuro-computational properties are expected to enable the design of new devices for applications in pattern recognition, signal analysis, associative memory and system control.

Our study is motivated by biological networks displaying rhythmic behaviour, such as the neocortex, hippocampus or olfactory bulb. Those networks have a functional organization based upon interactions within and among small populations of neurons. A common architectural feature of many natural neural systems is an anatomically distributed organization, hence neural computation requires that distinct structures communicate in a coordinated and modifiable fashion. Experimental evidence suggests that synchronous oscillations in the brain may be used to coordinate information processing in the nervous system [1]. Hence, an understanding of how oscillatory activity and transitions between different oscillatory states in neural networks arise is important for understanding the neuro-computational properties of such systems.

Oscillatory neural networks provide new paradigms for neural computation: neural oscillators are sensitive to the fine temporal structure (phase) of incoming signals (pulse trains). Like Hopfield networks, an oscillatory network possesses the ability of high-level cognitive functions, such as associative memory and pattern recognition. Memorized patterns in

0305-4470/00/183555+12$30.00

oscillatory neural networks correspond to synchronized states with prescribed phase relations. Pattern recognition is related to phase locking and associative recall by self-organization of the network [2–6]. Recently, Terman and Wang [7, 8] proposed a novel neural architecture based on competition and cooperation between locally excitatory and globally inhibitory populations of relaxation oscillators. They assumed that perceptual organization is based on the representation of oscillatory correlation: each object is represented by a synchronized oscillator population corresponding to the object and different objects are represented by different oscillator populations which are desynchronized from each other. Terman and Wang proved that global synchronization is a robust property of the local coupling. The global inhibitory mechanisms produced rapid desynchronization among different oscillator groups. Within this framework they solved computational problems such as image segmentation or object selection.

Oscillatory neural networks for pattern recognition, processing and storage could be implemented, for example, as electronic circuits based on classical neuronal oscillators, phase-locked loop (PLL) circuits, optical (laser) oscillators, superconducting Josephson junction oscillators or micro-electromechanical systems (MEMS). Micro-electromechanical systems are miniature mechanical systems, which are integrated with CMOS electronics [9–11]. Typically, MEMS are used for wireless communication and signal processing [12, 13]. The mechanical part senses external, non-electronic signals, such as for example barometric pressure, temperature, acceleration, vibration, etc, and the electronic part digitizes and processes the signals. The main part is the MEMS resonator, a polycrystalline silicon oscillator. Such an oscillator is described by

$$m\ddot{x} + f(x)\dot{x} + g(x) = 0 \tag{1}$$

where x denotes the displacement of the shuttle of the MEMS resonator from the rest position $x = 0$. The constant m is its effective mass, and $f(x)$ and $g(x)$ describe the damping and stiffness functions. Their exact form depends on the properties of the materials and details of the feedback loop circuitry (see [10] for detailed information about the electro-mechanics of MEMS). Second-order equations of the form (1) are known as Liénard equations, which are a generalization of the van der Pol oscillator.

In this paper we study dynamics and pattern formation in a hierarchical network of coupled bistable van der Pol oscillators. Bistability naturally arises in natural and artificial information processing systems, allowing coexisting attractors and transitions between different states of activity. To measure synchronization and disorder in distributed neural networks we apply the bi-orthogonal decomposition into empirical orthogonal spatial and temporal modes [14, 15]. The bi-orthogonal decomposition characterizes the dynamics by global, temporal and spatial entropy and energy. Previously, we applied this method on networks composed of Hopf-type oscillators and FitzHugh–Nagumo neural oscillators [16–18]. We found that the characteristic quantities of the bi-orthogonal decomposition are adequate parameters to characterize the complex dynamics of coupled nonlinear oscillators and neural networks. Different states of network activity can be identified as synchronous or asynchronous activity [16–18]. In addition, the bi-orthogonal decomposition detects bifurcations following variations of the system parameters.

2. An oscillatory neural network

2.1. The bistable van der Pol oscillator

Motivated by bistable MEMS oscillators [6, 19] in the following we study a network composed of van der Pol oscillators:

$$\ddot{x} + \varphi(x)\dot{x} + \omega^2 x = 0.$$

To obtain bistable dynamics, e.g. a rest state and an oscillating state which are simultaneously stable for the same set of parameters, the nonlinear damping term $\varphi(x)$ is replaced by a fourth-degree polynomial, i.e

$$\ddot{x} + \left(\varepsilon_1 - x^2\right)\left(\varepsilon_2 - x^2\right)\dot{x} + \omega^2 x = 0. \tag{2}$$

The bifurcation analysis of (2) was investigated in detail elsewhere [20]. We recall that in the weakly nonlinear limit, i.e. $\varepsilon_1, \varepsilon_2 \ll 1$, for $\varepsilon_2 > (3+\sqrt{8})\varepsilon_1$ and $0 < \varepsilon_1\varepsilon_2 \ll \omega$ we obtain an attractive fixed point at the origin and a pair of stable/unstable limit cycles with radii

$$r_{u,s} = \left(\frac{1}{\varepsilon_1\varepsilon_2}\left[\varepsilon_1 + \varepsilon_2 \pm \left(\varepsilon_1^2 + \varepsilon_2^2 - 8\varepsilon_1\varepsilon_2\right)^{1/2}\right]\right)^{1/2}. \tag{3}$$

2.2. Network topology

The topology (see figure 1) of our network is organized as a chain of eight clusters of oscillators, each cluster containing 16 oscillators. Within each cluster the oscillators are identical, and the internal coupling is global (all-to-all). In analogy with 'realistic' neuronal networks, the oscillators of each cluster are linked through activatory or inhibitory connections [17, 18]. The couplings are chosen as linear and symmetric over the y-components, i.e.

$$\dot{x}_i = y_i$$
$$\dot{y}_i = \left(x^2 - \varepsilon_1\right)\left(\varepsilon_2 - x^2\right)y_i - \omega^2 x_i + K_i.$$

Depending on the sign of the coupling term K_i, each cluster consists of four inhibitory and 12 excitatory oscillators, e.g. in the brain 10–25% of the neurons are inhibitory local circuit neurons. For an inhibitory oscillator i the coupling is given by

$$K_i = \frac{k_{nn}}{N-1}\sum_{k\neq i}^{N} y_k + \frac{k_{np}}{P}\sum_{j}^{P} y_j + k_{\mathrm{inp}}y_{\mathrm{inp}} \tag{4}$$

with $k_{nn} < 0$ and $k_{pn} > 0$. Here N labels the inhibitory and P labels the excitatory elements within a single cluster. All inhibitory and four excitatory oscillators receive external input, which is provided by an additional oscillator with frequency ω_{inp} and coupling strength k_{inp}. Within each cluster four excitatory oscillators are coupled to the corresponding oscillators of the neighbouring clusters. Thus, for both types of excitatory oscillators we have

$$K_i = \frac{k_{pp}}{P-1}\sum_{k\neq i}^{P} y_k + \frac{k_{np}}{N}\sum_{j}^{N} y_j + k y_l \tag{5}$$

with $k_{pp} > 0$ and $k_{np} < 0$. The index l denotes both an external oscillator, i.e. $k = k_{\mathrm{inp}} > 0$, or an oscillator l from a neighbouring cluster, i.e. $k = k_{cc} > 0$. Finally, the coupling terms of the remaining purely internal coupled oscillators are

$$K_i = \frac{k_{pp}}{P-1}\sum_{k\neq i}^{P} y_k + \frac{k_{np}}{N}\sum_{j}^{N} y_j \tag{6}$$

with $k_{pp} > 0$ and $k_{np} < 0$. Due to the different coupling terms the system may be regarded as consisting of four different types of oscillators. According to the topology described above, the labelling of the oscillators is organized as follows: the oscillators 0–31 are inhibitory elements, 32–63 are excitatory elements, both with external input, 64–91 are excitatory elements with input from the neighbouring cluster and 92–127 are the remaining excitatory elements. In the figures we denote these types (in the same order as above) with capital letters A–D.

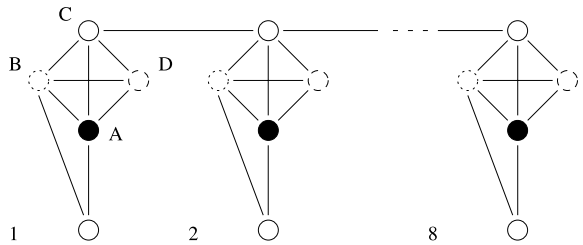

Figure 1. Schematic network topology. Organized as a chain of clusters of coupled oscillators, each circle represents an oscillator population as defined by the network connectivity: the population (A) are inhibitory oscillators and the populations (B)–(D) are exitatory oscillators. An external input is received by the populations (A) and (B). The population (C) provides interactions between neighbouring clusters.

3. Spatio-temporal data analysis

3.1. The bi-orthogonal decomposition

The decomposition into orthogonal modes is a well known procedure in signal analysis. A signal can be decomposed and represented in a new basis, such as via a Fourier or wavelet transform. Instead of using a predefined basis, the basis can be generated by the signal itself, which is referred to as empirical orthogonal decomposition, Karhunen–Loève transformation, singular-value decomposition or principal-component analysis. The bi-orthogonal decomposition is a spatio-temporal extension of the Karhunen–Loève transformation for the identification of coherent structures in turbulent systems and consists of a decomposition into spatial and temporal orthogonal modes [14, 15]. We refer to [14] for theoretical details of the method. Here we recall some notation and summarize the main results in the context of coupled oscillators. Any complex signal $u(z, t)$ on two variables may be decomposed uniquely as

$$u(z,t) = \sum_{n=1}^{N} \alpha_n \psi_n(t)\, \varphi_n(z) \tag{7}$$

where $\alpha_1 \geqslant \alpha_2 \geqslant \cdots \alpha_N \geqslant 0$ are the so-called singular values and φ_n and ψ_n are orthogonal functions [14]. The signal can then be identified with a linear operator $U : L^2(T) \to L^2(Z)$. Here, $L^2(T)$ consists of functions $t \to \psi(t)$ over the time domain. Formally, one may also consider t to be a continuous variable. In these cases $\psi(t)$ has to be square integrable. Analogously, $L^2(Z)$ is the space of functions $z \to \varphi(z)$. The spatial and temporal eigenfunctions $\varphi_n(z)$ and $\psi_n(t)$ satisfy $(\varphi_k, \varphi_l) = (\psi_k, \psi_l) = \delta_{kl}$ and are eigenfunctions of, respectively, $\boldsymbol{L} = U^t U$ and $\boldsymbol{R} = U U^t$, which are non-negative, self-adjoint operators in $L^2(Z)$ and $L^2(T)$ and represent the spatial and temporal correlation matrices of the signal. The corresponding eigenvalues are then just the squares of the singular values, i.e.

$$\boldsymbol{L}\varphi_n = \alpha_n^2 \varphi_n \qquad \boldsymbol{R}\psi_n = \alpha_n^2 \psi_n.$$

Due to the spatio-temporal symmetry of the decomposition, i.e. $L^t = R$, the eigenvalues α_k^2 are the same for both temporal and spatial eigenfunctions. The products $\varphi_n \psi_n$ are therefore referred to as independent coherent structures that compose the signal. The analysis of the signal then corresponds to the spectral analysis of the operator U associated with the signal $u(z, t)$.

Given a system of $\tilde{N}$ coupled oscillators with an individual oscillator consisting of s components, we interpret the evolution of the system as a spatio-temporal signal $u(x,t)$. Here, $x \in X = \{x_1, \ldots, x_N\}$ labels both the location and the component of an oscillator, i.e. X plays the role of the spatial domain. For our system, $\tilde{N} = 128$ and $s = 2$, hence $N = s\tilde{N} = 256$. Since the time evolution is determined by numerical integration, the time domain is also discrete, $t \in T = \{t_1, \ldots, t_M\}$. When the data $u(x,t)$ are arranged in the form of an $M \times N$ matrix, in our case N is less than M, the spectrum consists of N non-negative, singular values α_n.

3.2. Entropy, energy and dimension

Three types of characteristic quantities can be extracted from the bi-orthogonal decomposition: entropy, energy and dimension. The information content of a signal can be estimated by the entropy, which measures the degree of order of the spatio-temporal components of the signal. The global mode entropy is defined by

$$S(u) = -\frac{1}{\ln N}\sum_{k=1}^{N} p_k \ln p_k \tag{8}$$

with

$$p_k = \frac{\alpha_k^2}{\sum_k^N \alpha_k^2}.$$

The temporal and spatial entropies are defined by

$$S_T(x) = -\frac{1}{\ln N}\sum_{k=1}^{N} p_k(x) \ln p_k(x) \tag{9}$$

$$S_X(t) = -\frac{1}{\ln N}\sum_{k=1}^{N} p_k(t) \ln p_k(t) \tag{10}$$

where

$$p_k(x) = \frac{\alpha_k|\varphi_k(x)|}{\sum_k^N \alpha_k|\varphi_k(x)|} \qquad p_k(t) = \frac{\alpha_k|\psi_k(t)|}{\sum_k^N \alpha_k|\psi_k(t)|}.$$

The entropies are normalized by $0 \leqslant S \leqslant 1$. The amount of the global entropy depends on the number of non-zero eigenvalues. The entropy is maximal, $S = 1$, if all eigenvalues are equal, i.e. $p_k = 1/N$. If there is exactly one non-zero eigenvalue, that is, the energy is characterized by the first eigenmode alone, the entropy S will be zero.

The square norm of the signal in $L^2(X \times T)$ defines the global energy

$$E(u) = \sum_{x,t} u(x,t)^2 = \sum_{k=1}^{N} \alpha_k^2 \tag{11}$$

as the sum of the eigenvalues. The spatial and temporal energies are defined as

$$E_X(t) = \sum_{x} u(x,t)^2 = \sum_{k=1}^{N} \alpha_k^2 |\psi_k(t)|^2 \tag{12}$$

and

$$E_T(x) = \sum_{t} u(x,t)^2 = \sum_{k=1}^{N} \alpha_k^2 |\varphi_k(x)|^2. \tag{13}$$

Since the bi-orthogonal decomposition is generated from a solution $u(x,t)$ of a dynamical system, the eigenfunctions and eigenvalues contain information on the attractor of the system. Hence one could formally define a global dimension as the dimension of the range of U, i.e. dim $\leqslant N$, which is the effective number of degrees of freedom of the signal. However, the number of non-zero eigenvalues is the dimension of the smallest linear subspace containing the dynamics and consequently only an upper bound for the fractal or correlation dimension of the attractor. For our study we use the working definition that the dimension is given by the number of actual eigenfunctions required so that the captured energy is at least 90% of the total energy.

4. Simulations

For all oscillators within the network we choose the parameters $\epsilon_1 = 0.1, \epsilon_2 = 0.6$ and $\omega = 1.0$ out of the bistable regime. External input is provided by oscillators with parameters $\epsilon_1 = -0.1$ and $\epsilon_2 = 0.8$. The coefficients for the coupling strengths are given by $k_{pp} = -k_{nn} = 0.01$, $k_{np} = -k_{pn} = -0.02$ and $k_{cc} = 0.02$. To minimize boundary effects, the couplings between clusters 1 and 2, 7 and 8 are set to $k_{cc}/4$ and between clusters 2 and 3, and 6 and 7 to $k_{cc}/2$.

The stable steady-state solution is $x_i = 0$, $y_i = 0$ for all i. Since we are interested in oscillatory solutions, we choose random starting values for $r_i = (x_i^2 + y_i^2)^{1/2}$ from the interval [0.8, 1.2], which is the basin of attraction for the stable limit cycle of the free oscillator. The phases are chosen randomly out of the interval $[0, \pi/2]$.

We investigated the dynamics while the frequency of the external oscillator was varied from $\omega_{\text{inp}} = 0.1$ to $\omega_{\text{inp}} = 3.5$ with a step width of 0.01 and the external coupling strength was varied from $k_{\text{inp}} = 0.1$ to 1.0 with a step width of 0.1. The numerical integration was performed using a Runge–Kutta algorithm with an adaptive step size. For the calculations of the global characteristics and the bi-orthogonal decomposition the system was first integrated for a transient time of 1000 time steps ($t_1 = 0$ to $t_2 = 1000$). Then from $t_2 = 1000$ to $t_3 = 1300$ the calculated values were stored at 512 equidistant time steps to obtain a spatio-temporal time series, which was used for further analysis.

4.1. Dynamics without external input

The dynamics of globally coupled bistable oscillators or systems with nearest-neighbour couplings (such as chains and arrays) is well understood [20–22]. The bistability may result in non-trivial spatio-temporal dynamics. Depending on the choice of parameter values and initial conditions the network without external input also shows different types of collective behaviour. For purely excitatory couplings the network totally synchronizes in-phase after a short transient. The global energy is maximal for this case ($E = 148.6$). Incorporating different inhibitory connectivity the network remain synchronized, but typically we found antiphase synchronization either between the excitatory and inhibitory populations, or between a single cluster and the other clusters. We also observed a lower amount of global energy. In contrast, global entropy and dimension are almost constant, i.e. $S \approx 0.13$ and dim $= 2$.

This behaviour in the absence of external input can be explained by the ability of coupled oscillators near Hopf bifurcation to synchronize, which is discussed in detail in [2]. Applying the transformation $\omega y = -\dot{x} - \phi(x)$ we obtain a first-order differential equation in Liénard form

$$\dot{x} = -\omega y - \phi(x)$$

$$\dot{y} = -\frac{1}{\omega}\left[\ddot{x} + \phi'(x)\dot{x}\right] = \omega x$$

with

$$\phi(x) = \int_0^x \mathrm{d}s\, \varphi(s) = \varepsilon_1\varepsilon_2 x - \tfrac{1}{3}(\varepsilon_1 + \varepsilon_2)x^3 + \tfrac{1}{5}x^5.$$

An energy estimate for the uncoupled equations is provided by

$$\frac{\mathrm{d}}{\mathrm{d}t}\tfrac{1}{2}\left(x^2 + y^2\right) = -x^2\left[\varepsilon_1\varepsilon_2 - \tfrac{1}{3}(\varepsilon_1 + \varepsilon_2)x^2 + \tfrac{1}{5}x^4\right].$$

From this we can easily find a Lyapunov function for the network which guarantees the existence of stable attractors and the asymptotic behaviour to recall memorized patterns (see [9]).

4.2. Synchronized and desynchronized patterns induced by external input

The onset of external input changes the global activity of the network, which can be observed in figure 2 in the plots for global energy and entropy, $E(\omega_{\mathrm{inp}}, k_{\mathrm{inp}})$ and $S(\omega_{\mathrm{inp}}, k_{\mathrm{inp}})$, respectively. We can observe three main regions of the dynamics: the main resonance $\omega_{\mathrm{inp}}/\omega = 1$, subharmonic resonances and higher harmonic resonances. In the main resonance at $\omega_{\mathrm{inp}}/\omega = 1$ global entropy and dimension are minimal. Since synchronized states are characterized by minima of the global entropy $S(k_{\mathrm{inp}}, \omega_{\mathrm{inp}})$, respectively, maxima of the global energy $E(k_{\mathrm{inp}}, \omega_{\mathrm{inp}})$, for resonant input the network behaves as without external input. The dimension is dim $= 2$ and the global entropy $S \approx 0.13$. The global energy increases with external input strength.

Subharmonic resonances can be observed at $\omega_{\mathrm{inp}}/\omega = 0.34$ and 0.22, as well as higher harmonics at multiples of the resonance frequency. In all resonances the global entropy has a global or local minimum, indicating a high degree of coherence. Close to the resonances the global entropy increases, indicating disordered or chaotic activity. Increasing the strength of internal couplings, the synchronized range of the main resonance broadens (see figure 3), which can be explained by the shape of the entrainment domains ('Arnold tongues') for coupled nonlinear oscillators [23, 24]. We can also observe a local minima of the global entropy near the main resonance, which will be studied in the next section.

For input frequencies $\omega_{\mathrm{inp}} > \omega$ we observe an increase of global entropy for increasing input strength until $k_{\mathrm{inp}} \approx 0.5$. For stronger input the entropy decreases again. We omit further details on synchronized and desynchronized patterns, since this was studied in detail in our previous work [16–18]. Note that for resonant input the network has the properties of an oscillatory associative memory. Dephased input on the excitatory and inhibitory populations results in dephasing the different populations. The phase relationships depend on the choice of the connection matrix. Generally, for all parameter values the dynamics converges to an attractor, random initial conditions for fixed parameter result in the same oscillatory patterns.

4.3. Bifurcations

We can use the global entropy as an order parameter allowing to locate and follow bifurcations [15]. The variation of the global entropy as a function ω_{inp} and k_{inp} is well understood from the theoretical finding that the entropy can be increased by internal or external bifurcations. Internal bifurcations are characterized by a constant dimension. The resulting peculiar dynamics is explained by rotations of the space and time eigendirections in the degenerate eigenspaces and a reordering of the coherent structures. In contrast, external bifurcations are characterized by an increase of dimension. Bifurcations are observed as mode crossings of the eigenvalues,

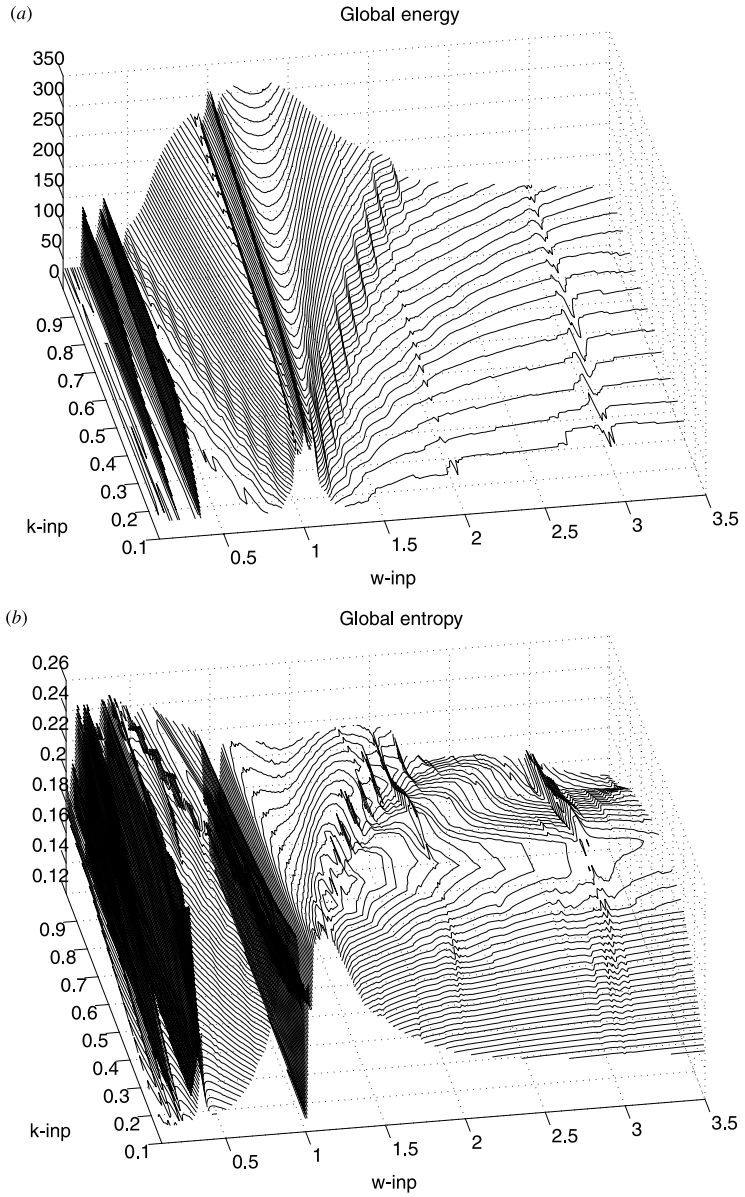

Figure 2. Global energy E and entropy S for varying external input frequency ω_{inp} and input strength k_{inp}.

giving rise to an exchange of the coherent structures. New modes may became dominant and more modes are simultaneously active.

This can be observed in figure 3 where the four dominant eigenvalues are shown. In figures 2 and 3 we can observe that mode crossings occur for $\Delta = \omega_{\text{inp}} - \omega \approx k_{\text{inp}}$. This is in good agreement with our theoretical predictions for two coupled oscillators near degenerate Hopf bifurcation. In the bistable range the unstable/stable pair of limit cycles may coalesce and vanish as a result of detuning the frequencies of the oscillators or by varying coupling strength

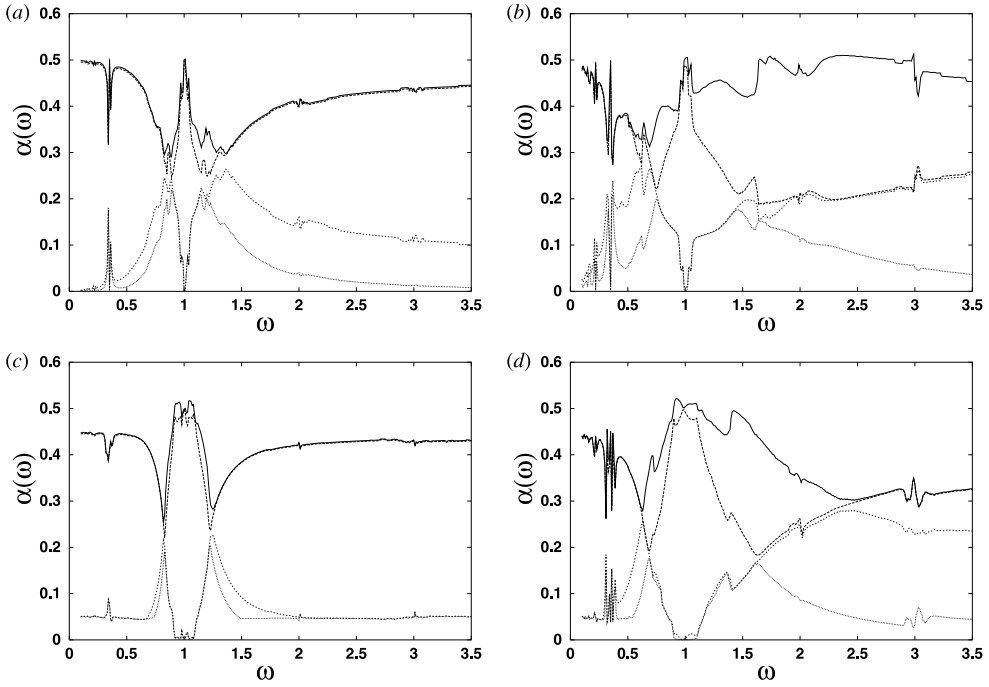

Figure 3. Dominant eigenvalues $\alpha_i(\omega_{\rm inp})$ for (*a*) external input strength $k_{\rm inp} = 0.1$, (*b*) external input strength $k_{\rm inp} = 0.5$. In (*c*) and (*d*) we show the dominant eigenvalues for (*c*) external input strength $k_{\rm inp} = 0.1$, and (*d*) external input strength $k_{\rm inp} = 0.5$ for increased internal couplings $k_{pp} = k_{nn} = 0.1$, $k_{np} = -k_{pn} = -0.2$, and $k_{cc} = 0.2$.

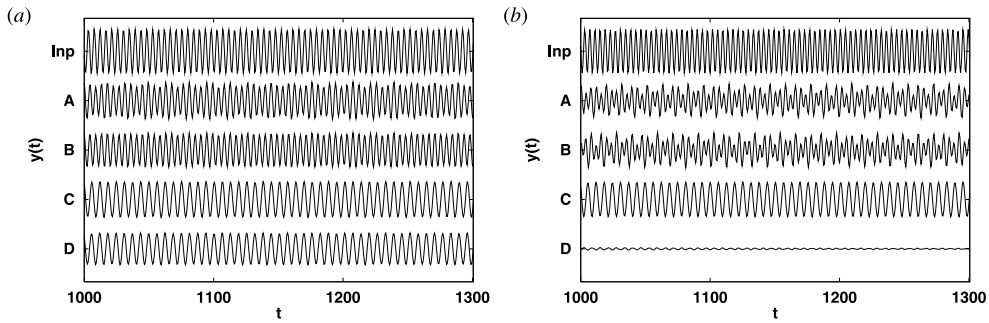

Figure 4. Oscillatory patterns $y_i(t)$ for one oscillator of each population at $k_{\rm inp} = 0.5$ and (*a*) $\omega_{\rm inp} = 1.4$, (*b*) $\omega_{\rm inp} = 1.6$

[25]. We can observe mode crossings which corresponds to this bifurcation, for example, for $k_{\rm inp} = 0.5$ in the range between $\omega_{\rm inp} = 1.5$ and 1.6. For $\omega_{\rm inp} = 1.5$ the eigenvalues α_3 and α_4 are degenerate, then α_3 increases and α_4 decreases. For $\omega_{\rm inp} > 1.6$ α_2 and α_3 are degenerate. An increase of the internal coupling strengths does not change the qualitative dynamics (see figures 3(*c*) and (*d*). Increasing the coupling strengths between oscillators of population D no mode crossings were observed for weak external input, i.e. $k_{\rm inp} \ll k_{cc}$, due to the competition between external input and input from the neighbouring clusters.

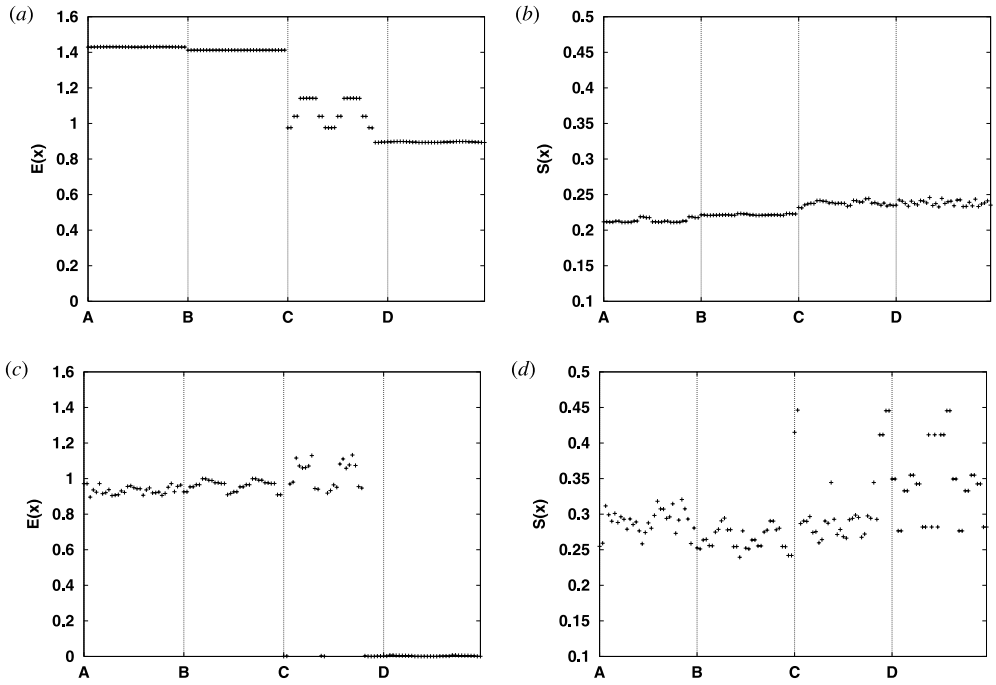

Figure 5. (a) Temporal energy and (*b*) temporal entropy for $k_{\mathrm{inp}} = 0.5$ and $\omega_{\mathrm{inp}} = 1.4$. (*c*) Temporal energy and (*d*) temporal entropy for $k_{\mathrm{inp}} = 0.5$ and $\omega_{\mathrm{inp}} = 1.6$. For $\omega_{\mathrm{inp}} = 1.4$ the different populations show a high degree of coherence. The loss of coherence for $\omega_{\mathrm{inp}} = 1.6$ indicate irregular or chaotic dynamics.

A detailed analysis of the network dynamics near the mode crossings shows that the temporal energy decreases, indicating a decrease in the amplitudes of the oscillators (see figures 4 and 5). At $\omega_{\mathrm{inp}} = 1.5$ the oscillators of population D contribute especially to the qualitative change of the dynamics, they cease to oscillate with small-amplitude fluctuations near their stable rest states. The spatial entropy increases, indicating increasing disorder or desynchronization. We can observe two main regimes of the dynamics under non-resonant input. Generally, the oscillators receiving external input adapt the frequency of the external forcing. Depending on the state of population D, i.e. oscillatory or at rest, there is regular or chaotic dynamics of the input populations A and B. The oscillators of population C show the most regular behaviour. They oscillate with their intrinsic frequencies without any significant amplitude modulations. The additional cluster–cluster connections seem to stabilize this population. The distribution of the spatial energies of population C in figures 5(*a*) and (*c*) reflects the symmetry properties of the network, i.e. the decaying coupling strengths towards the network boundaries. This, in turn, may explain the fact that some oscillators of this population show small-amplitude fluctuations as a boundary effect.

4.4. Low-dimensional dynamics

From the bi-orthogonal decomposition we obtain a network dynamics which is governed by a low-dimensional dynamical system. Both the unforced network and synchronized states under external input are characterized by two eigenmodes containing about 98% of the global energy and minimal global entropy. Depending on the input frequency and coupling strength

the dimension varies between dim = 2 and 8. Increasing the number of oscillators within each cluster does not change the network dynamics. The numerical values of global entropy and energy vary with network size and parameter values. However, modifying the network size by incorporating additional clusters even in different organizational schemes such as larger chains or two-dimensional arrays of clusters does not change the qualitative spatio-temporal properties of the network.

5. Summary and discussion

Weakly connected neuronal oscillators near Hopf bifurcation are sensitive to the timing of incoming signals [2]. The phase of one oscillator can affect the other only when both oscillators have resonant frequencies. As a result, oscillators with different frequencies do not interact via phase deviations even though they are interconnected. Therefore, in order to achieve communication between two neural oscillators they must establish a common frequency of transmission. Thus, an oscillator can interact selectively with other oscillators having appropriate frequencies. External input can serve to dynamically connect or disconnect two oscillators [4, 25].

The main findings of our investigations are that depending on the detuning between internal frequency and input frequency, external input with an appropriate frequency and strength results in asynchronous network dynamics. In addition, by applying the bi-orthogonal spectral decomposition on the spatio-temporal data obtained from the network, we can detect saddle-node bifurcations of the unstable/stable pair of limit cycles in larger ensembles of bistable oscillators by varying input frequency and strength. As shown previously for two coupled oscillators near degenerate Hopf bifurcation [25], this behaviour can be observed just below the critical coupling for synchronization and results in an attraction of the dynamics to the stable steady state. In contrast to the Hopf-type oscillators used in [16], some results may be explained by the relaxation nature of the oscillation. Relaxation oscillators typically synchronize in-phase and can also interact for low-order resonant frequencies. This may explain the increasing global energy for subharmonic resonances.

These properties are of great importance in artificial and biological signal processing systems. The biological relevance of the presented network is discussed in detail in [16]. We note that our network may serve as an abstract thalamo-cortical system, providing an input layer receiving sensory information and a layer of cortical columns. In a real cortex the cortical columns have output layers with feedback connections from cortical neurons to the reticular nucleus of the thalamus. These feedback connections are not implemented in the present network, however, their effects on the network dynamics may be briefly considered. The reticular cells inhibit thalamic relay cells supplying adjacent cortical columns, thus forming a large system of multiple parallel loops (thalamic relay cells, cortical column, reticular thalamic cells, thalamic relay cells). Adjusting the internal and external coupling strength in our network determines the sensitivity of these loops to input frequency. A non-resonant input results in the observed bifurcation in population D. Using this population as an output layer, it provides feedback for resonant input which may allow us to implement mechanisms for gating of information or selective attention. Thus we expect to obtain similar computational properties of the network presented here to those of the networks proposed by Terman and Wang [7, 8]. This will be the subject of further investigations.

The bi-orthogonal decomposition is a useful tool in analysing the dynamics of coupled nonlinear oscillators even in heterogeneous topologies and intermediate ensembles. Besides insight into the dynamics and bifurcations of the system, the low-dimensional description by the bi-orthogonal decomposition provides advantages for a detailed analysis using simplified

systems (see, for example, [16]). It may also be useful in designing and optimizing networks by finding a suitable size for given applications. Computer simulations give easy access to parameter values, initial conditions and the evolution of the system. Since the method is based on spatio-temporal data obtained from the system, it may also be used for experimental data, i.e. for testing and quality control of hardware implementations such as, for example, of MEMS oscillators. Using bistable oscillators for neural network simulations and applications provides the possibility for a more biologically realistic description of neuronal activity. They may also enable the design of interfaces between new oscillatory neural networks and classical, binary computer systems. An advantage of using relaxation oscillators to perform computational tasks is their ability of rapid synchronization, mediated by the so-called fast threshold modulation [26].

References

[1] Gray C M 1994 *J. Comput. Neurosci.* **1** 11
[2] Hoppensteadt F C and Izhikevich E M 1997 *Weakly Connected Neural Networks* (Berlin: Springer)
[3] Hoppensteadt F C and Izhikevich E M 1998 *BioSystems* **48** 85
[4] Hoppensteadt F C and Izhikevich E M 1999 *Phys. Rev. Lett.* **82** 2983
[5] Hoppensteadt F C and Izhikevich E M 1999 Synchronization of laser oscillators, associative memory and optical neurocomputing *Phys. Rev.* E submitted
[6] Izhikevich E M 1999 Computing with oscillators *Neural Networks* submitted
[7] Terman D and Wang D L 1995 *Physica* D **81** 148
[8] Wang D L and Terman D 1997 *Neural Comput.* **9** 805
[9] Hoppensteadt F C and Izhikevich E M 1999 Synchronization of MEMS resonators and mechanical neurocomputing *IEEE Trans. Circuits Syst.* I submitted
[10] Nguyen C T C and Howe R T 1999 *IEEE J. Solid-State Circuits* **34** 440
[11] Turner K L, Miller S A, Hartwell P G, MacDonald N C, Strogatz S H and Adams S G 1998 *Nature* **396** 149
[12] Mason A, Yazdi N, Chavan A V, Najafi K and Wise K D 1998 *Proc. IEEE* **86** 1733
[13] Yazdi N, Ayazi F and Najafi K 1998 *Proc. IEEE* **86** 1640
[14] Aubry N, Guyonnet R and Lima R 1991 *J. Stat. Phys.* **64** 683
[15] Aubry N, Guyonnet R and Lima R 1992 *J. Nonlinear Sci.* **2** 183
[16] Schwarz J, Sieck A, Dangelmayr G and Stevens A 2000 *Biol. Cybern.* **82** 231
[17] Schwarz J, Stevens A, Bräuer K and Bartels M 2000 Patterns of complexity and coherent oscillations in a thalamo-cortical network model *Chaos in Brain?* ed K Lehnartz *et al* (Singapore: World Scientific) pp 238–42
[18] Schwarz J, Stevens A, Bräuer K and Bartels M 1999 Modulation of synchrony in a thalamo-cortical network model *Preprint*
[19] Wang Y C, Adams S G, Thorp J S, MacDonald N C, Hartwell P and Bertsch F 1998 *IEEE Trans. Circuits Syst.* **45** 1013
[20] Defontaines A, Pomeau Y and Rostand B 1990 *Physica* D **46** 201
[21] Mackay R S and Sepulchre J A 1995 *Physica* D **82** 243
[22] Nekortin V I, Makarov V A, Kazanetsev V B and Velarde M G 1997 *Physica* D **100** 330
[23] Chicone C 1992 *SIAM J. Math. Anal.* **23** 1577
[24] Chicone C 1994 *J. Diff. Eq.* **112** 407
[25] Schwarz J, Dangelmayr G, Stevens A and Bräuer K 1999 Burst and spike synchronization of coupled neural oscillators *Dyn. Stab. Syst.* submitted
[26] Somers D and Kopell N 1995 *Biol. Cybern.* **68** 393